Vol 26 (3)

Ingeniería y Competitividad
Vol 26 (3) 2024; doi: 10.25100/iyc.v26i3.14343

ISSN
0123-3033
e- 2027-8284

Original Article

Wavelet Analysis of a High Impedance Fault Modeled as a Stochastic Hybrid SystemProducts

Análisis Wavelet de un fallo de alta impedancia modelado como un Sistema Híbrido Estocástico

Guillermo Gallo[1] Wilder Herrera[1] Juan D. Mina-Casaran[1]

[1]Rynova Research Group, Rymel Ingeniería Eléctrica S.A.S., Copacabana, Colombia.

How to cite?

Gallo, G., Herrera, W., Mina-Casaran, J.D. Wavelet Analysis of a High Impedance Fault Modeled as a Stochastic Hybrid System Products. Ingeniería y Competitividad, 2024, 26(3)e-21614343.

https://doi.org/10.25100/iyc.v26i3.14343

Recibido: 19-07-24
Evaluado: 20-09-24
Aceptado: 24-10-24
Online: 21-11-24

Correspondence
direccioninnovacion@rymel.com.co

Abstract

Introduction: electrical networks are sensitive to faults, and among the most common types, one of the most difficult to detect is the High Impedance Fault (HIF). This type of fault can go unnoticed due to its particular characteristics, such as the ground resistance and voltage drops in the electric arc.
Objective: to propose a stochastic hybrid model for simulating high impedance faults, using the Ornstein-Uhlenbeck process to describe the random nature of these faults. The model focuses on key HIF parameters: ground resistance and voltage drops in the electric arc.
Methodology: the Ornstein-Uhlenbeck process is used to model the randomness of high impedance faults. Simulations are conducted to compare the numerical results with experimental signals reported in the literature. Additionally, both continuous and discrete wavelet transforms are applied to the line current signal to analyze fault characteristics.
Results: the simulations show a qualitative similarity between the numerical results obtained and the experimental signals available in the literature. Both continuous and discrete wavelet transforms reveal typical features of high impedance faults, validating the effectiveness of the proposed model.
Conclusions: the proposed stochastic hybrid model for high impedance faults is effective in simulating this type of fault, and wavelet transform analyses demonstrate its ability to identify distinctive characteristics of HIFs, which can improve the detection and diagnosis of these faults in electrical networks.

Keywords: high Impedance Fault, Stochastic Hybrid System, Stochastic Process, Continuous Wavelet Transform, Discrete Wavelet Transform.

Resumen

Introducción: las redes eléctricas son sensibles a fallas, y entre las principales, una de las más difíciles de detectar es la Falla de Alta Impedancia (HIF, por sus siglas en inglés). Este tipo de fallas puede pasar desapercibido debido a sus características particulares, como la resistencia a tierra y las caídas de voltaje en el arco eléctrico.
Objetivo: proponer un modelo híbrido estocástico para la simulación de fallas de alta impedancia, utilizando el proceso de Ornstein–Uhlenbeck para describir la naturaleza aleatoria de estas fallas. El modelo se enfoca en los parámetros clave de las HIF: la resistencia a tierra y las caídas de voltaje en el arco eléctrico.
Metodología: se utiliza el proceso de Ornstein–Uhlenbeck para modelar la aleatoriedad de la falla de alta impedancia. Se realizan simulaciones que permiten comparar los resultados numéricos con señales experimentales reportadas en la literatura. Además, se aplican transformadas de wavelet tanto continuas como discretas sobre la señal de corriente de línea para analizar las características de las fallas..
Resultados: las simulaciones muestran una similitud cualitativa entre los resultados numéricos obtenidos y las señales experimentales disponibles en la literatura. Se observa que tanto en la transformada de wavelet continua como en la discreta, aparecen características típicas de las fallas de alta impedancia, lo que valida la efectividad del modelo propuesto..
Conclusiones: el modelo híbrido estocástico propuesto para fallas de alta impedancia es efectivo en la simulación de este tipo de fallas, y los análisis mediante transformadas de wavelet demuestran su capacidad para identificar características distintivas de las HIF, lo que puede mejorar la detección y el diagnóstico de estas fallas en redes eléctricas.

Palabras clave: falla de alta impedancia, sistema híbrido estocástico, proceso estocástico, transformada wavelet continua, transformada wavelet discreta.

Why was it done?
IThe study was conducted to address the detection of high-impedance faults (HIF), which pose a significant risk to human, animal, and environmental safety. Given that these faults are challenging to detect and testing them under real-world conditions can be costly and dangerous, the study aimed to develop new algorithms and methods for their detection. In this context, simulation emerges as a useful tool but requires suitable models that reflect the random nature of these faults. Therefore, the authors focused on creating a stochastic model to emulate the random behavior of HIFs.
What were the most relevant results?
The most relevant results of the study include the development of a stochastic model based on an Ornstein-Uhlenbeck process, which successfully reproduced HIF signals similar to experimental ones. This model enabled time and frequency analysis using wavelet transforms, revealing characteristics of HIFs that may be useful for the development of detection algorithms. In particular, an increase in high-frequency power was observed during fault occurrences, providing valuable insights into the behavior of these faults under simulated conditions.
What do these results provide?
The findings provide a solid foundation for future research and developments in HIF detection. By offering an accurate mathematical model to represent the random variation of fault parameters, this study paves the way for the experimental calibration and validation of the model. Moreover, the combination of wavelet analysis with a stochastic model could facilitate the training of neural networks for HIF detection, offering an innovative and efficient approach to improving safety in electrical systems.

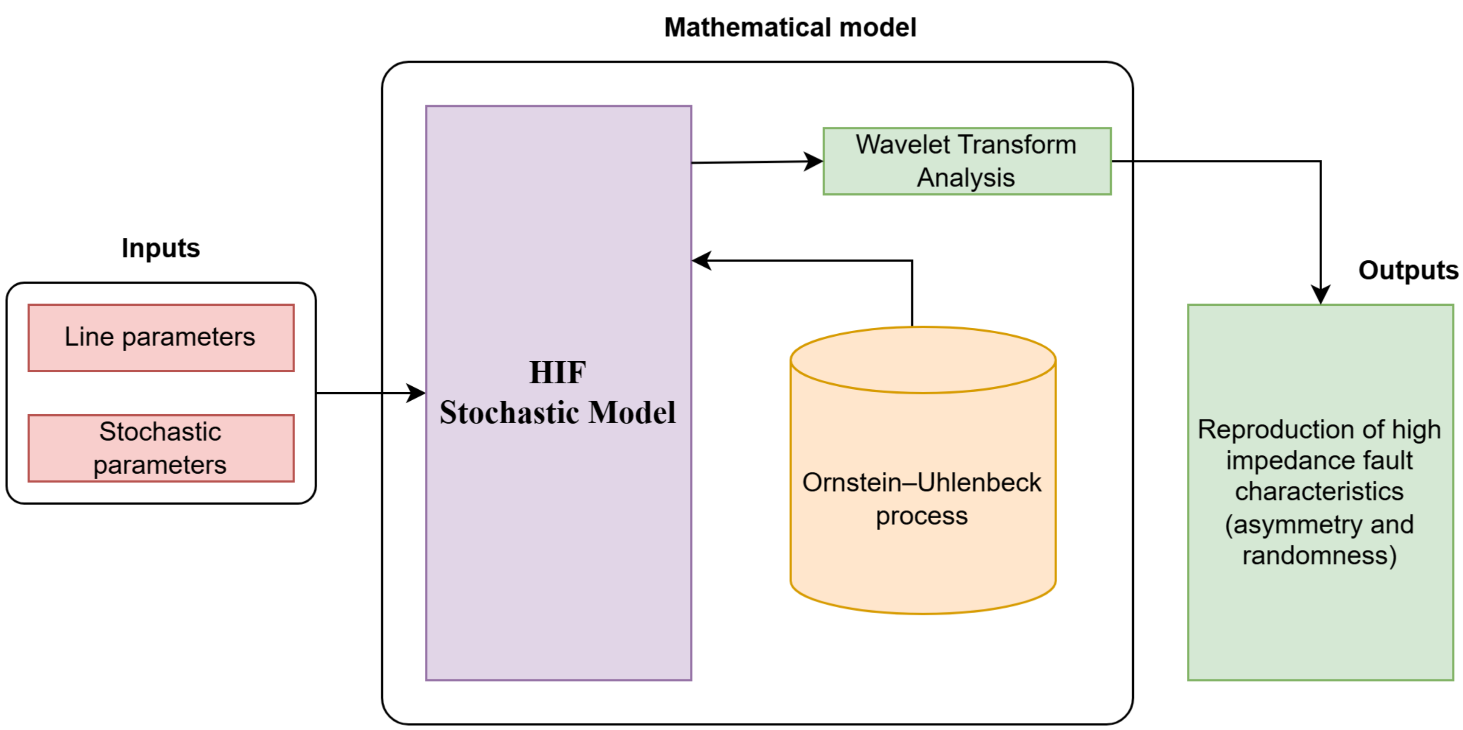

doi: 10.25100/iyc.v26i3.14343

Introduction

Electrical networks are sensitive to faults. Among the main faults, one of the most difficult ones to detect is the High Impedance Fault (HIF) (1,2). HIFs do not represent a threat to electrical equipment (3). However, since this fault is characterized by the presence of electrical arcs it represents a high risk to people, animals and vegetation (4). HIF occurs when a conductor, broken or unbroken, makes contact with a high impedance surface, such as a high impedance ground surface, a deteriorated insulator or a tree branch (5). Given the high impedance of the contact surfaces, the currents generated by this type of fault are insufficient to activate the conventional over-current protection devices (6). Also, other characteristics of HIFs include asymmetry, randomness, build-up, shoulder, and intermittency (7).

Due to the difficulty of detecting HIFs, different detection techniques based on analysis in the domain of time, frequency and time-frequency have been proposed (8). One of the most used techniques today is the Wavelet Transform (WT) (9). WT is a tool that allows to analyze the behavior of a signal in the domain of the time and frequency (10). This tool is widely used for the analysis and detection of the HIFs due to its non-stationary behavior.

Both real and simulated data are used to develop detection algorithms based on the WT and other techniques (11). Carrying out real experiments poses a high risk to power grids; it is very difficult to carry out experiments where the appearance of several simultaneous faults is contemplated. In addition, collecting real data represents some associated monetary costs. However, the study of complex scenarios can be done more easily in a simulated way (12).

Therefore, it is necessary to carry out a modeling stage as a step before performing simulations. The modeling of HIFs has been the cornerstone of several researches (5,7,11). One of the first approximations for a model was proposed by Emanuel in (13), which is presented in Figure 1. This model uses diodes and DC sources to explain voltage drops due to electrical arcs. It also explains some non-linear characteristics of the current signals. In this case, a distortion is generated through the diodes, which physically represents the zero conduction moments. One of the characteristics that is not clearly defined in Emanuel's model is randomness. There are some works that, using models-based Emanuel's model and circuits simulators, have recreated a random behavior (11,12,14). However, no analytical explanation of this behavior is reported.

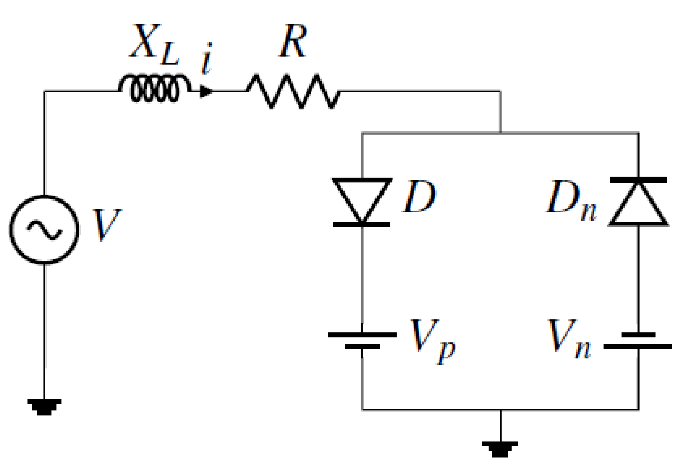

Figure 1. Emanuel's Model

There is a another potentially complex situation in the modeling process that Emmanuel's model could arise. Due to the presence of diodes, a set of circuit topologies is generated. Each topology depends on the state of the diodes (on, off). The number of topologies is $2n$; where n is the number of diodes (15). However, not all topologies have to be presented in a simulation, some of

doi: 10.25100/iyc.v26i3.14343

them are physically impossible. An alternative for modeling systems that change topology is hybrid systems (16). They are complex dynamical systems that combine the interaction of continuous and discrete dynamics. Each continuous system is governed by a continuous vector field represented through a system of ordinary differential equations. The discrete dynamics are usually represented by graphs, finite state machines or automata.

Although hybrid systems have been used successfully for the modeling, simulation, and control of complex systems, they cannot reproduce the random characteristics of some processes (17). As a response to this lack, stochastic hybrid systems have been proposed. This kind of system adds random uncertainty to the processes. These random uncertainties can be added to the systems of equations in the form of Wiener processes, generating a Stochastic Differential Equations System (SDES) (18).

In this paper, a stochastic approach for modeling HIFs is presented. The proposed model is generated from some Emanuel-based models. Unlike some previously reported studies, this model offers an explanation for the randomness of the fault parameters by means of stochastic differential equations. The proposed model is presented as a hybrid stochastic automaton. Some simulations are carried out in order to show the qualitative similarity between the results generated by the proposed model and the experimental results reported in the literature. Finally, the continuous and discrete Wavelet transform has been applied to the simulation results in order to show the appearance of the fault in the time-frequency domain and to demonstrate the susceptibility of this model to generate proper characteristics of the HIFs.

The rest of the content in this article is distributed as follows. In section 2, a complete description of the mathematical modeling of a HIF using hybrid systems, SDES, and Wiener processes, is presented. Section 3 presents the Wavelet Analysis of the system. In Section 4 a discussion on HIF models is addressed. Finally, some conclusions are listed in Section 5.

Mathematical Modeling and Simulation

Consider a single-phase power distribution line like the one illustrated in Fig. 2(a). Some similar line models have been used in (19). This model considers a distributed capacitances equal to $\frac{C}{2}$ in parallel with the source and the fault to give it a bit more realism. In addition, the total capacitance is C.

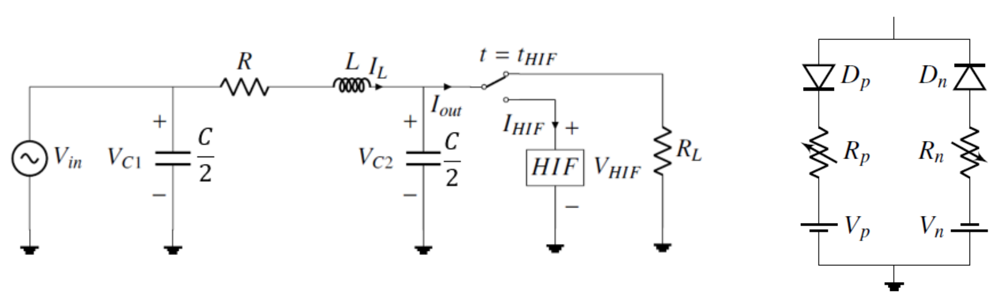

(a) (b)

Figure 2. Model of a power line affected by a high impedance fault: (a) Line model, (b) HIF model.

The selected HIF model is based on the Emanuel model (13) and it is depicted in Fig. 2(b). This model has already been widely reviewed in the literature (20–24). The physical meaning of the parameters is as follows: R_p and R_n represent the ground resistance, V_p and V_n represent the voltage drop in the electric arc. During a time of the positive half cycle, the current flows through D_p, R_p, and V_p. Likewise, during a time of the negative half cycle, the current flows through D_n, R_n

doi: 10.25100/iyc.v26i3.14343

and V_n. This model reproduces some typical characteristics of high impedance faults such as non-linearity and asymmetry in currents (1). The main disadvantage of this type of model is that it must be empirically verified (8).

By analyzing the circuit in Figure 2 using Kirchhoff's voltage and current laws, a mathematical model of the system can be obtained. $Let\ X = [V_{C1}, I_L, V_{C2}]$ and $V_{in} = A\ sin(\omega t)$. Therefore, HIF can be modeled with the following system of ordinary differential Equations (1) to (3):

$$\begin{cases} dX_1 = A\omega \cos(\omega t)dt \\ dX_2 = \dfrac{1}{L}(X_1 - RX_2 - X_3)dt \\ dX_3 = \dfrac{1}{C}(X_2 - I_{out})dt \end{cases} \tag{1}$$

where I_{out} is the output current and it can vary according to whether the system is operating normally ($t < t_{HIF}$) or if the fault has occurred ($t \geq t_{HIF}$). I_{out} is defined as follows:

$$\begin{cases} \dfrac{X_3}{R_L}\ if\ t < t_{HIF} \\ I_{HIF}\ if\ t \geq t_{HIF} \end{cases} \tag{2}$$

where I_{HIF} is the current of the HIF and it is defined as follows:

$$\begin{cases} 0\ if\ V_p > X_3 > -V_n\ \vee\ t < t_{HIF} \\ \dfrac{X_3 - V_p}{R_p}\ if\ X_3 \geq V_p\ \wedge\ t \geq t_{HIF} \\ \dfrac{X_3 + V_n}{R_n}\ if\ X_3 \leq -V_n\ \wedge\ t \geq t_{HIF} \end{cases} \tag{3}$$

Although the model in Equation (1) can represent the non-linearity and asymmetry characteristic of HIF, it cannot represent their stochastic nature. There are works that have addressed the issue of randomness in HIF. In an attempt to recreate this behavior, some studies have used circuit simulation software and statistic switches (25). Another strategy consists of randomly varying the R_p and R_n values (26). Other works vary randomly both the value of the resistors and the value of the DC sources (24). Although the random nature of high impedance faults has already been recreated in the studies cited above, none of these articles offer a complete explanation of randomness modeling. Next, one of the main contributions will be presented, which is the approach of a stochastic model, to explain the variation of the parameters.

Stochastic Modeling of the HIF parameters

It is observed in the literature that the normal distribution has been used to represent the random behavior of resistance to earth and electric arc (27,28). With this in mind, Gaussian processes can be proposed to model R_p, R_n, V_p, and V_n. The Ornstein–Uhlenbeck process model is known to be a Gaussian stochastic process with applications in physics (29), electrical engineering (30), financial mathematics (31), and other disciplines (32). Consider the Ornstein–Uhlenbeck process represented by Equation (4):

$$dX = \theta(\mu - X)dt + \sigma dW \tag{4}$$

The stochastic process is also known as the Vasicek model, and it is used in financial mathematics to describe the evolution of interest rates (33). In this model, W stands for a Wiener process, μ is the long-term mean, θ is the speed of reversion to the mean and σ is the instantaneous volatility. Vasicek model is useful for representing variables that do not drift toward infinity, but instead

doi: 10.25100/iyc.v26i3.14343

oscillate around a mean value, μ. The term $\theta\,(\mu - X)$ is known as instantaneous drift, it is the force that pulls the process towards the long-term mean. On the other hand, the stochastic term σdW is a white noise with variance σ^2. This term causes the process to oscillate erratically around the long-term mean.

Based on the Vasicek model, a stochastic process is proposed for modeling the parameters (R_p, R_n, V_p, and V_n) of a HIF. Consider the SDES representing by Equation (5):

$$\begin{cases} dR_p = \theta_R(\mu_R - R_p)dt + \sigma_R dW_1 \\ dR_n = \theta_R(\mu_R - R_n)dt + \sigma_R dW_2 \\ dV_p = \theta_V(\mu_V - V_p)dt + \sigma_V dW_3 \\ dV_n = \theta_V(\mu_V - V_n)dt + \sigma_V dW_4 \end{cases} \quad (5)$$

Note that Equation (5) consists of a system of 4 independent equations. The stochastic variables are assumed to evolve independently; however, in a future work, some link could be generated between them. Also note that for simplicity, the same parameters have been assumed for dR_p and dR_n, in the same way for dV_p and dV_n. It could also be interesting to use different parameters to model the behavior of the components of the positive half cycle (R_p and V_p) and the components of the negative half cycle (R_n and V_n); this could accentuate some typical characteristics of HIF, such as asymmetry.

Stochastic Hybrid System

Hybrid systems are a kind of dynamical system that combine the interaction of continuous and discrete dynamics. Continuous dynamics are time-driven, while discrete ones are event-driven (18). One way of understanding hybrid systems is through a state machine or automaton, a hybrid automaton. In this type of automaton, each discrete state contains a continuous system, usually modeled by a system of differential equations. The transitions between the different discrete states are given by the evolution of the continuous variables.

Hybrid systems have been applied for the modeling, analysis, and control of complex systems. This type of model does not give rise to uncertainties, given the deterministic nature of the equations it contains. However, there are processes and systems with uncertain behaviors in the real world, and this is when the use of stochastic models is necessary. There are several ways to add randomness to a hybrid model. One way is to add it to the continuous models, generating SDES. Another way is to add uncertainty to the transition rules between the different states. The last way is by adding uncertainty to both the continuous models and the transition rules (16). In this work, the first way will be addressed, where uncertainty will be added to the different continuous models that represent the HIF. Thanks to this, a set of SDES can be obtained.

By analyzing the HIF model of Figure 2 and the Equations (2) and (3), it is observed that four different circuit topologies or states can be presented. The four states are depicted in Figure 3.

doi: 10.25100/iyc.v26i3.14343

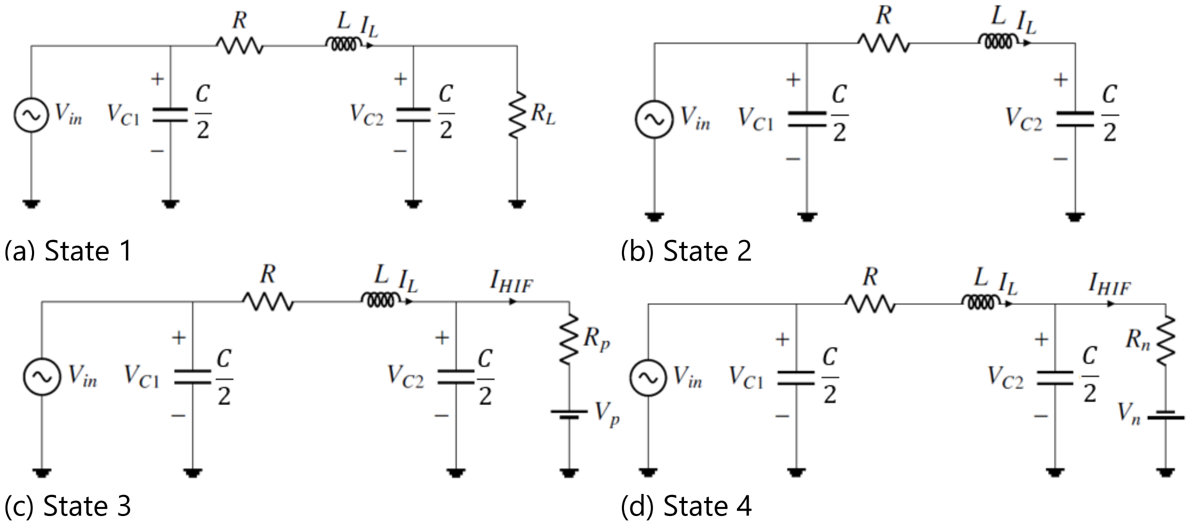

Figure 3. Circuit Topologies

The first state represents the operation of the system in the absence of fault. In the second state, there is no HIF current flow ($I_{HIF} = 0$), since the voltage is not sufficient to generate an electric arc. In the other two states there is an HIF current, since the voltage is sufficient to generate an electric arc. The third state corresponds to a current flow in the positive half cycle, while the fourth state is for the negative half cycle. By taking Equations (1), (2), (3) and adding the random dynamics for the HIF parameters proposed in Equation (5), a stochastic differential equation system can be proposed for each of the four states. $Let\ X = V_{C1}, I_L, V_{C2}, R_p, R_n, V_p, V_n$ and $V_{in} = A\sin(\omega t)$. Next, a stochastic model for each state from Equation (6) to (9), is defined:

State 1. The system operates without fault, $t < t_{HIF}$.

$$\begin{cases} dX_1 = A\omega\cos(\omega t)dt \\ dX_2 = \frac{1}{L}(X_1 - RX_2 - X_3)dt \\ dX_3 = \frac{1}{C}(X_2 - \frac{1}{R_L}X_3)dt \\ dX_4 = \theta_R(\mu_R - X_4)dt + \sigma_R dW_1 \\ dX_5 = \theta_R(\mu_R - X_5)dt + \sigma_R dW_2 \\ dX_6 = \theta_V(\mu_V - X_6)dt + \sigma_V dW_3 \\ dX_7 = \theta_V(\mu_V - X_7)dt + \sigma_V dW_4 \end{cases} \quad (6)$$

State 2. There is a fault, but no current flow through the fault, $t \geq t_{HIF}$ and $I_{HIF} = 0$.

$$\begin{cases} dX_1 = A\omega\cos(\omega t)dt \\ dX_2 = \frac{1}{L}(X_1 - RX_2 - X_3)dt \\ dX_3 = \frac{1}{C}X_2 dt \\ dX_4 = \theta_R(\mu_R - X_4)dt + \sigma_R dW_1 \\ dX_5 = \theta_R(\mu_R - X_5)dt + \sigma_R dW_2 \\ dX_6 = \theta_V(\mu_V - X_6)dt + \sigma_V dW_3 \\ dX_7 = \theta_V(\mu_V - X_7)dt + \sigma_V dW_4 \end{cases} \quad (7)$$

doi: 10.25100/iyc.v26i3.14343

State 3. Fault current flow in the positive half cycle, $t \geq t_{HIF}$.

$$\begin{cases} dX_1 = A\omega\cos(\omega t)dt \\ dX_2 = \dfrac{1}{L}(X_1 - RX_2 - X_3)dt \\ dX_3 = \dfrac{1}{C}\left(X_2 - \dfrac{1}{X_4}(X_3 - X_6)\right)dt \\ dX_4 = \theta_R(\mu_R - X_4)dt + \sigma_R dW_1 \\ dX_5 = \theta_R(\mu_R - X_5)dt + \sigma_R dW_2 \\ dX_6 = \theta_V(\mu_V - X_6)dt + \sigma_V dW_3 \\ dX_7 = \theta_V(\mu_V - X_7)dt + \sigma_V dW_4 \end{cases} \quad (8)$$

State 4. Fault current flow in the negative half cycle, $t \geq t_{HIF}$.

$$\begin{cases} dX_1 = A\omega\cos(\omega t)dt \\ dX_2 = \dfrac{1}{L}(X_1 - RX_2 - X_3)dt \\ dX_3 = \dfrac{1}{C}\left(X_2 - \dfrac{1}{X_5}(X_3 + X_7)\right)dt \\ dX_4 = \theta_R(\mu_R - X_4)dt + \sigma_R dW_1 \\ dX_5 = \theta_R(\mu_R - X_5)dt + \sigma_R dW_2 \\ dX_6 = \theta_V(\mu_V - X_6)dt + \sigma_V dW_3 \\ dX_7 = \theta_V(\mu_V - X_7)dt + \sigma_V dW_4 \end{cases} \quad (9)$$

Now four SDES associated with four different states have been determined. Therefore, the complete system can be modeled through a stochastic hybrid automaton, as illustrated in Figure 4.

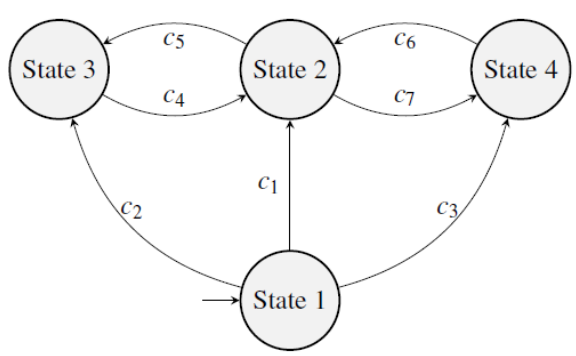

Figure 4. Stochastic Hybrid Automaton

Conditions c_1, c_2, c_3 and c_4 determine transitions between states and are event-driven. They are defined below:

$c_1: t = t_{HIF} \land X_6 > X_3 > -X_7$, a fault occurs but the line voltage is insufficient to generate an electric arc.

$c_2: t = t_{HIF} \land X_3 \geq X_6$, a fault occurs and the line voltage is higher than the arc voltage on the positive half cycle.

doi: 10.25100/iyc.v26i3.14343

$c_3{:}t = t_{HIF} \wedge X_3 \leq -X_7$, a fault occurs and the line voltage is lower than the arc voltage on the negative half cycle.

$c_4{:}X_3 - X_6 = 0 \downarrow$, the line voltage drops until it reaches V_P. The down arrow denotes the decreasing direction of the event.

$c_5{:}X_3 - X_6 = 0 \uparrow$, the line voltage rises until it reaches V_P. The up arrow denotes the increasing direction of the event.

$c_6{:}X_3 + X_6 = 0 \uparrow$, the line voltage rises until it reaches $-V_n$.

$c_7{:}X_3 + X_7 = 0 \downarrow$, the line voltage drops until it reaches $-V_n$.

Simulations

To numerically test the performance of the proposed stochastic model, some simulations have been carried out. The SDES were integrated using the algorithm proposed in (34). A medium voltage line was simulated with the following parameters: $A = 4400\sqrt{6}[V], \omega = 120\pi\ rad, R = 0.1\ [\Omega], L = 1.3\ [mH], C = 18\ [nF], RL = 3593\ [\Omega]$. Regarding the stochastic parameters ($\theta_R, \theta_V, \mu_R, \mu_V, \sigma_R$ and σ_V), these were chosen by analyzing the ranges of variation used in (11), where simulations were carried out by randomly varying the resistance to earth from 150 [Ω] to 12 [kΩ] and the DC voltage associated with the electric arc from 1.5 kV to 10.5 kV. The mean value of the variation intervals was selected as the values of the long-term expected values, that is, $\mu_R = 6075$ and $\mu_V = 6000$. The other parameters were estimated keeping in mind the long-term variance of a Vacisek process. For the process described in Equation (4), the long-term variance is equal to $\frac{\sigma_2}{2\theta}$. The other stochastic parameters have been estimated in such a way that the long-term standard deviations are equal to half the lengths of the variation intervals. Based on the above, the following values have been chosen: $\theta_R = 1.28, \theta_V = 1.28, \sigma_R = 9480$ and $\sigma_V = 7200$. This study has assumed the previous values in order to demonstrate that the model can recreate the stochastic behavior of a HIF with greater qualitative proximity.

Figure 5 illustrates the stochastic behavior of the HIF parameters. Note that unlike a conventional Wiener process, these random walks evolve in the vicinity of the long-term expected values.

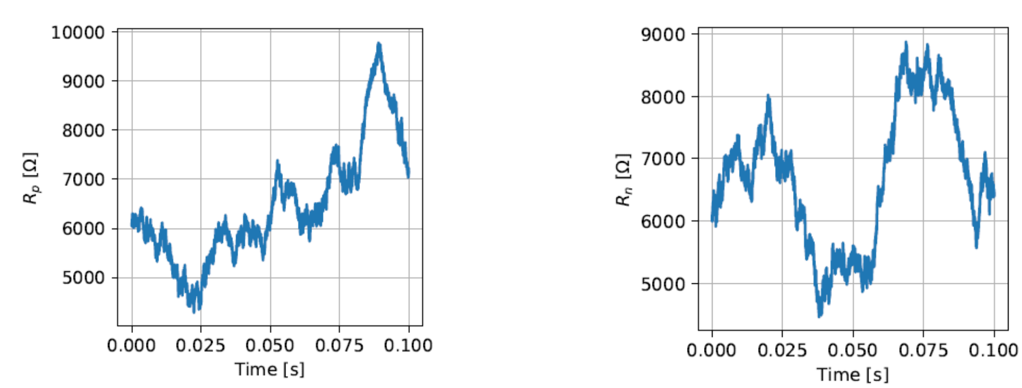

(a) R_p (b) R_n

doi: 10.25100/iyc.v26i3.14343

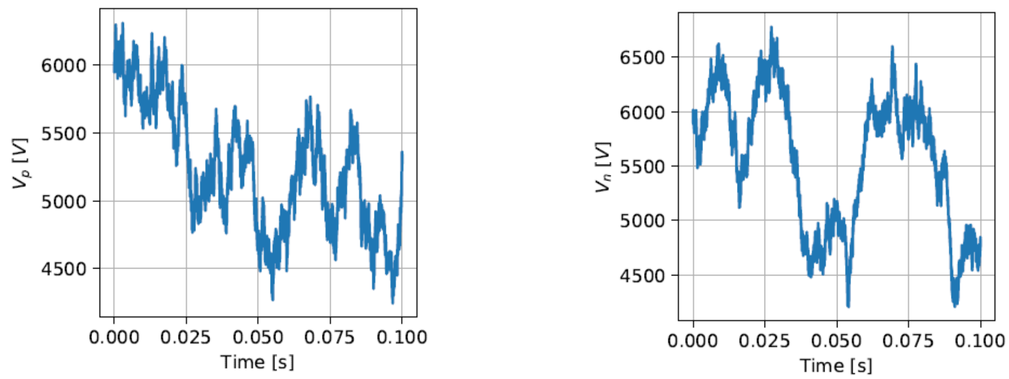

(c) V_p (d) V_n

Figure 5. Stochastic behavior of the HIV parameters

On the other hand, Figure 6 shows the random behavior of the line current. Two simulation scenarios have been considered. In the first, the fault occurs throughout the simulation period, $t_{HIF} = 0$. In the second scenario, the fault occurs in the middle of the simulation period, $t_{HIF} = 0.05$. Figures 6(a)(b) show the evolution of I_L, which represents the line current considering the leakage currents derived through the capacitance between the line and ground. On the other hand, Figures 6(c)(d) show the current of the HIF itself. It should be noted that in practice, the current that is most likely to be observed is I_L. It can be shown that the real fault currents obtained experimentally have a great qualitative similarity to those obtained with the stochastic model proposed in this work. For example, in (35) and (36), the experimentally obtained fault currents have great similarity in shape with IL. Even the small erratic oscillations of the current are reproduced by the proposed model. This is achieved thanks to stochastic modeling of resistance to ground. On the other hand, the arc voltage models (V_p and V_n) generate asymmetry in the current peaks.

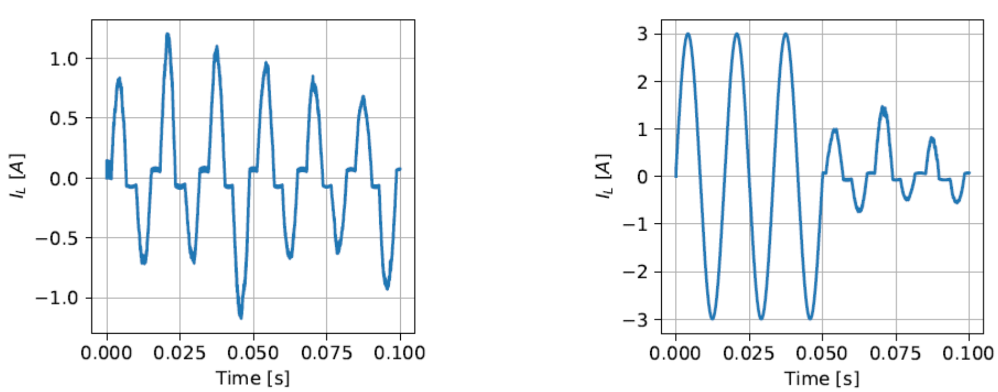

(a) $t_{HIF} = 0s$ (b) $t_{HIF} = 0.05s$

doi: 10.25100/iyc.v26i3.14343

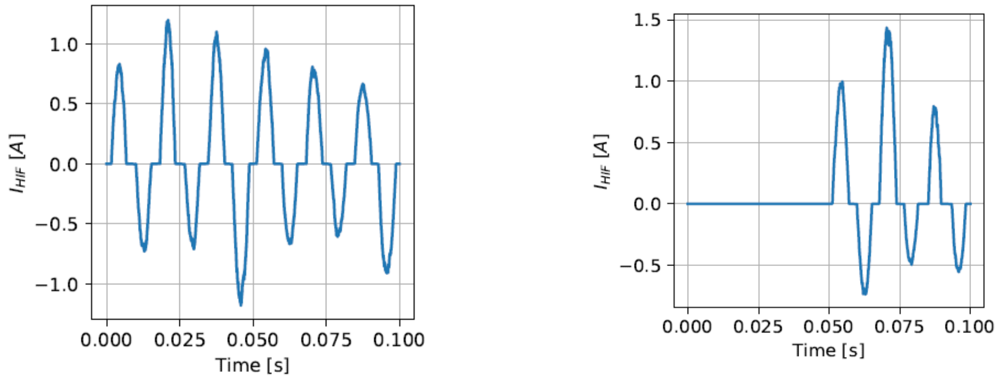

(c) $t_{HIF} = 0s$

(d) $t_{HIF} = 0.05s$

Figure 6. Stochastic behavior of the HIV currents

Figure 7 depicts the I-V characteristics. Figure 7(b) shows the characteristic generated by the HIF proposed model; it can be seen that it is qualitatively similar to that obtained by Emanuel (13). However, this characteristic curve would be very difficult to see in practice, unless the fault is reproduced in a laboratory environment, such as in (36). A characteristic curve that is easier to obtain in practice can be seen in Figure 7(a). In the central part of this curve, it can be seen that the current is not zero when the fault voltage is not enough to generate an electric arc. This effect can be explained with leakage currents, which in the model proposed in this work, are those currents that flow through the capacitance between the line and the ground. Other studies have reported similar characteristic curves (11,12,37).

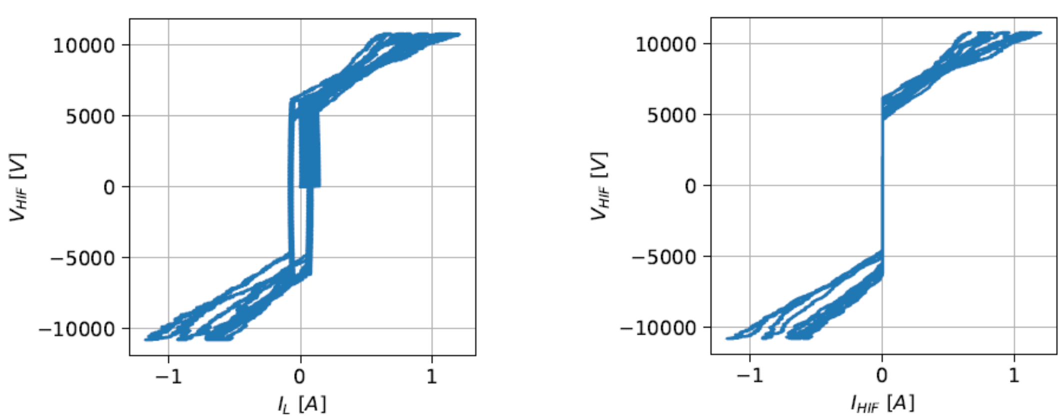

(a) I_L vs V_{HIF}

(b) I_{HIF} vs V_{HIF}

Figure 7. I-V Characteristics, $t_{HIF} = 0s$.

Wavelet Transform Analysis

WT generates a time-frequency representation of a signal. This property allows WT-based methods to adequately analyze signals with a time-varying spectrum, such as HIF current (8). Given the non-stationary nature of HIFs, WT is one of the most widely used tools for their analysis and detection. However, developing a systematic wavelet-based HIF detection algorithm is a challenging task. The most serious difficulties in using WT includes the subjectivity for choosing the mother Wavelet and narrow capability for high frequency analysis (38).

Unlike the Fourier Transform, WT uses wavelets instead of sines. Wavelets are families of functions generated from a single signal, the Mother Wavelet. Each of the wavelets are dilated and translated

doi: 10.25100/iyc.v26i3.14343

versions of the mother Wavelet. Dilation allows the mother wavelet to be scaled so that information on high and low frequencies can be obtained. On the other hand, translation is used to obtain time information. Wavelets are oscillatory signals that rapidly drop to zero; they are also differentiable, compact, and zero-mean (3). Figure 8 illustrates the wavelets used in this analysis.

(a) Complex Morlet (b) Daubechies

Figure 8. Continuous and Discrete Wavelets

WT analysis can be performed in two ways: Continuous Wavelet transform (CWT) or Discrete Wavelet transform (DWT). The purpose of this section is to perform both continuous and discrete wavelet analysis to the results obtained by the proposed stochastic model. This work seeks more than to generate a HIF detection technique to establish a reference framework for HIF modeling that could be used in future work for the training and adjustment of algorithms and models for HIF detection. To carry out these analyses, Python library called PyWavelets were used. CWT and DWT of the line current signal (I_L) were carried out, in order to appreciate the appearance of the HIF fault in the time-frequency domain.

Continuous Wavelet Transform Analysis

The CWT is defined such as is presented in Equation (10) (39):

$$CWT_{f(t)}(a,b) = \int_{-\infty}^{\infty} f(t)\frac{1}{\sqrt{a}}\overline{\psi\left(\frac{t-b}{a}\right)}dt \quad (10)$$

where $\psi(.)$ is the mother wavelet, which is continuously scaled by factor of a and continuously translated by factor of b. The so-called Complex Morlet Wavelet as a mother was used, as shown in Figure 8(a). By applying the transform to the current signal, the results illustrated in Figure 9 will be obtained. Figure 9(a) shows the results of the transform when the HIF occurs during the entire simulation time ($t_{HIF} = 0s$). It can be faintly seen that the highest concentration of signal power is around 60 Hz. In a more interesting situation, Figure 9(b) presents the results when the HIF is located in the second half of the simulation interval ($t_{HIF} = 0.05s$).

doi: 10.25100/iyc.v26i3.14343

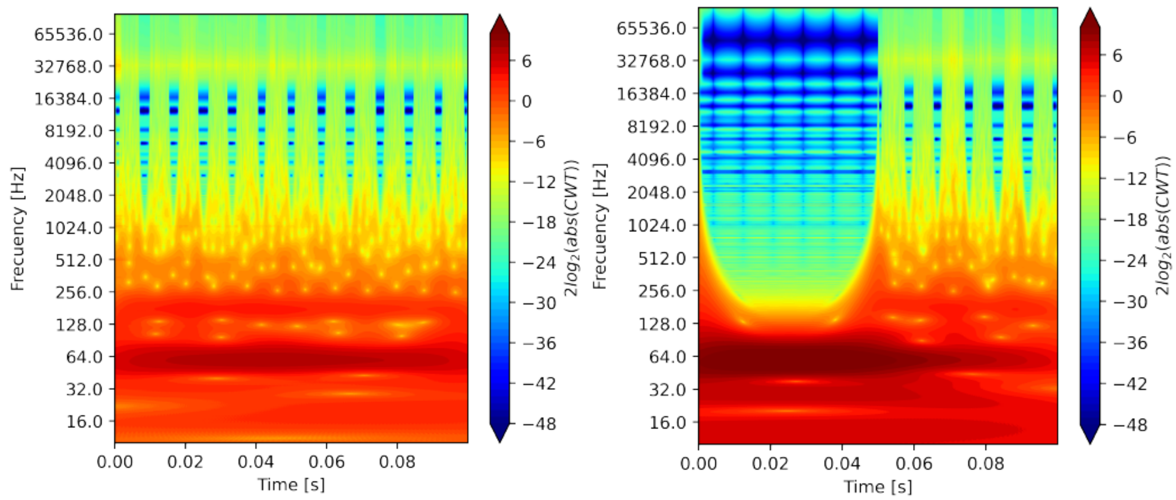

(a) $t_{HIF} = 0s$

(a) $t_{HIF} = 0.05s$

Figure 9. Spectrogram of IL

It can be clearly seen how the occurrence of the fault alters the spectrum. Although this type of analysis makes it possible to locate the occurrence of a HIF, its practical implementation in an electrical protection system is not very viable, given its computational cost.

Discrete Wavelet Transform Analysis

WT has one type of discrete implementation, the DWT. This type of transformation is often used for HIF detection due to its ease of implementation and its relatively low computational cost (3). The DWT of a signal $f(x)$ is defined as is presented in Equation (11) (40):

$$DWT_{f(t)}(m,n) = \frac{1}{\sqrt{a_0^m}} \sum_k f(k) \psi \overline{\left(\frac{n - k a_0^m}{a_0^m} \right)} \tag{11}$$

where $\psi(.)$ is a discrete mother wavelet, which is scaled by factor of a_0^m and translated by factor of ka_0^m. The above transformation is usually carried out by dilating the mother wavelet by a factor of two ($a_0 = 2$), which is known as the dyadic transformation (36,40).

The computational implementation of DWT is usually done using a filter bank, as illustrated in Figure 10. First, the discrete signal $f[n]$ is discomposed in a_1 and d_1 by means of a low pass filter $g[n]$ and a high pass filter $h[n]$, respectively. a_1 is called approximation of the signal and contains low frequency components. On the other hand, d_1 is known as signal details and contains high frequency components. Each stage is implemented with down sampling of the low-pass filter output. This feature makes it easier to calculate higher coefficients but limits the number of filtering levels to a maximum level of decomposition. Nevertheless, the implementation of a filter bank is computationally efficient (40).

doi: 10.25100/iyc.v26i3.14343

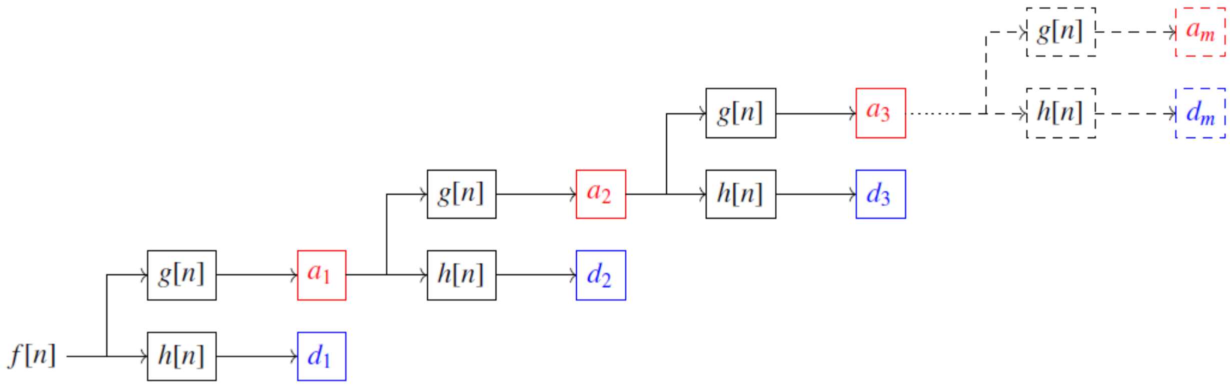

Figure 10. DWT as a filter bank.

The DWT to the current signal I_L up to the sixth level of decomposition, was carried out. For this, the well-known Daubechies as a mother wavelet, was used. It has been seen in the literature that this wavelet has been applied for the detection of HIFs. The main reasons for its wide use include powerful performance, easy implementation, sensitivity to signals with low amplitudes, low period, and fast decay. From the entire Daubechies family, the Daubechies wavelet 14 (db14) was selected, as in Figure 8(b).

Figure 11 illustrates the results of applying DWT to the line current, I_L. This study has analyzed the case where the HIF occurs in the middle of the simulation interval, $t_{HIF} = 0.05\ s$. Only the high frequency components were illustrated (details) because these coefficients are the ones commonly used in fault detection algorithms. It can clearly be seen how all the details begin to manifest just when the HIF appears. Some oscillation at the beginning can also be seen, but this is due to the simulation starting at $t = 0$, which implies an initial discontinuity; the electric signals did not come oscillating from $t < 0$.

doi: 10.25100/iyc.v26i3.14343

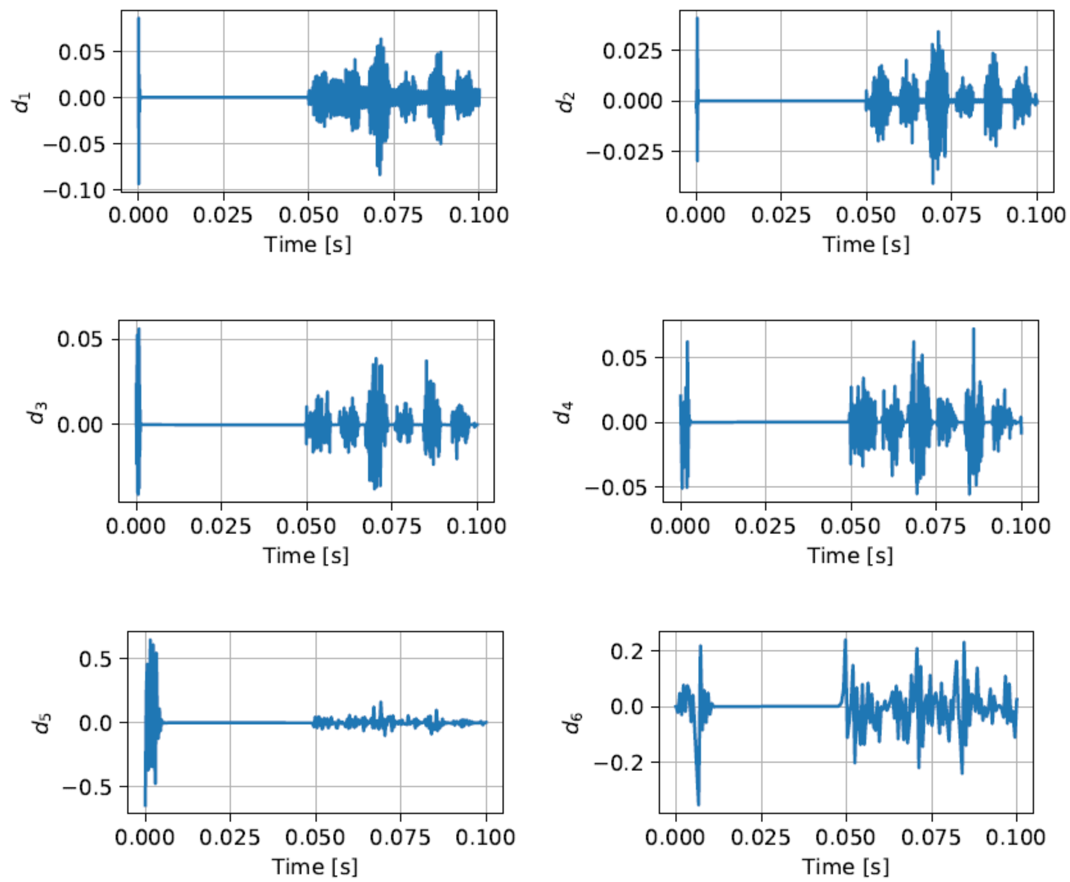

Figure 11. DWT, $\mathrm{tHIF} = 0.05\ \mathrm{s}$.

These results show that the DWT allows to distinguish between a normal behavior and a HIF, when a stochastic model is used to represent the HIF. It is important to note that the proposed model allows to represent the typical random dynamics of a HIF. Applying DWT to the data generated by model proposed in this work could generate characteristics more similar to those of a real HIF, which would allow better training algorithms for HIF detection.

Discussion

There are studies of random behavior of the electric arc parameters using Gaussian models. This is the reason for using a Gaussian process like the Ornstein–Uhlenbeck to model the HIF parameters. However, from the literature that has been searched, no explanatory mathematical model of the random variation of the HIF parameters has been found. This is the main contribution of this work. Most of the reported works use simulators such as PSCAD or MATLAB to perform numerical experiments. The task of modeling the entire system with equations was addressed, which was undoubtedly a more time-consuming task but one that gave us more control over the simulations. The continuous and discrete Wavelet transform has been applied to the line current data obtained with the proposed model. In both types of transforms, the appearance of the fault has been clearly evidenced. In the case of the CWT, it was observed in the spectrogram how when the fault occurred, the power of the high frequencies increased, while the fundamental frequency seemed to fade. On the other hand, through DWT, the high-frequency details were obtained up to the sixth

doi: 10.25100/iyc.v26i3.14343

level. It was possible to see how these coefficients took on significant values before the occurrence of the failure. Obtaining experimental data from a HIF is a difficult task. Given its cost and danger, it also limits the study cases according to the availability of elements to experiment. That is why the modeling and simulation of this electrical phenomenon takes on great meaning and value. The proposed model generates results that are qualitatively similar to the experimental ones and allows considering different scenarios for the fault. Additionally, given that the behavior of randomness through equations has been described, this model is susceptible to being adjusted and calibrated through experimental validation. The results of a stochastic model like this in conjunction with a morphological or wavelet analysis could provide better data to, for example, train a neural network for HIF detection. This is something that could be validated in future work.

Conclusion

A hybrid stochastic model has been proposed to represent HIFs. The model employs a SDES based on an Ornstein–Uhlenbeck process, specifically the Vasicek model. This model was used to represent the random behavior of the parameters of the HIF: resistance to ground and voltage drops in the electric arc. The proposed model reproduces some characteristics of high impedance faults such as asymmetry and randomness. A qualitative similarity was observed between the current signals obtained with the proposed model and some experimental results reported in the literature.

CRediT authorship contribution statement

Guillermo Gallo: conceptualization-ideas, data curation, formal analysis, research, methodology, software, validation, visualization-preparation, writing-original draft-preparation, writing-revision and editing-preparation. Wilder Herrera: conceptualization-ideas, data curation, formal analysis, funding acquisition, research, resources. Juan David Mina: formal analysis, funding acquisition, research, project management, resources, supervision, visualization-preparation, drafting, original draft-preparation, writing-revision and editing-preparation.

Conflicts of interest

No, the authors declare that they have no conflict of interest in the writing or publication of this article.

Ethical implications

No, the authors have no ethical implications to declare in the writing and publication of this article.

Financing

No, the authors declare that they received no resources for the writing or publication of this article.

doi: 10.25100/iyc.v26i3.14343

References

1. Bai H, Gao JH, Li W, Wang K, Guo MF. Detection of High-Impedance Fault in Distribution Networks Using Frequency-Band Energy Curve. IEEE Sens J [Internet]. 2024 Jan 1;24(1):427–36. Available from: https://ieeexplore.ieee.org/document/10316233/

2. Grimaldi RBG, Chagas TSA, Montalvão J, Brito NSD, dos Santos WC, Ferreira T V. High impedance fault detection based on linear prediction. Electr Power Syst Res [Internet]. 2021 Jan;190(August 2020):106846. Available from: https://doi.org/10.1016/j.epsr.2020.106846

3. Gomes DPS, Ozansoy C. High-impedance faults in power distribution systems: A narrative of the field's developments. ISA Trans [Internet]. 2021 Dec;118(xxxx):15–34. Available from: https://doi.org/10.1016/j.isatra.2021.02.018

4. Huaquisaca Paye JC, Vieira JPA, Tabora JM, Leão AP, Cordeiro MAM, Junior GC, et al. High Impedance Fault Models for Overhead Distribution Networks: A Review and Comparison with MV Lab Experiments. Energies [Internet]. 2024 Feb 27;17(5):1125. Available from: https://www.mdpi.com/1996-1073/17/5/1125

5. Mahari A, Seyedi H. High impedance fault protection in transmission lines using a WPT-based algorithm. Int J Electr Power Energy Syst [Internet]. 2015 May;67:537–45. Available from: http://dx.doi.org/10.1016/j.ijepes.2014.12.022

6. Langeroudi AT, Abdelaziz MMA. Preventative high impedance fault detection using distribution system state estimation. Electr Power Syst Res [Internet]. 2020 Sep;186(November 2019):106394. Available from: https://doi.org/10.1016/j.epsr.2020.106394

7. Aljohani A, Habiballah I. High-Impedance Fault Diagnosis: A Review. Energies [Internet]. 2020 Dec 5;13(23):6447. Available from: https://www.mdpi.com/1996-1073/13/23/6447

8. Ghaderi A, Ginn HL, Mohammadpour HA. High impedance fault detection: A review. Electr Power Syst Res [Internet]. 2017 Feb;143:376–88. Available from: http://dx.doi.org/10.1016/j.epsr.2016.10.021

9. Makkawi B, Usta Ö. High Impedance Fault Detection in Medium Voltage Distribution Systems Using Wavelet Transform. Turkish J Electr Power Energy Syst [Internet]. 2024 Mar 5;4(1):40–9. Available from: https://tepesjournal.org/en/high-impedance-fault-detection-in-medium-voltage-distribution-systems-u-wavelet-transform-1361

10. Bhongade S, Golhani S. HIF detection using wavelet transform, travelling wave and support vector machine. In: 2016 International Conference on Electrical Power and Energy Systems (ICEPES) [Internet]. IEEE; 2016. p. 151–6. Available from: http://ieeexplore.ieee.org/document/7915922/

11. Sekar K, Mohanty NK. Data mining-based high impedance fault detection using mathematical morphology. Comput Electr Eng [Internet]. 2018 Jul;69(May):129–41. Available from: https://doi.org/10.1016/j.compeleceng.2018.05.010

doi: 10.25100/iyc.v26i3.14343

12. Sedighi A. A New Model for High Impedance Fault in Electrical Distribution Systems. Int J Sci Res Comput Sci Eng Res [Internet]. 2014;2(4):6–12. Available from: www.isroset.org

13. Emanuel AE, Cyganski D, Orr JA, Shiller S, Gulachenski EM. High impedance fault arcing on sandy soil in 15 kV distribution feeders: contributions to the evaluation of the low frequency spectrum. IEEE Trans Power Deliv [Internet]. 1990 Apr;5(2):676–86. Available from: http://ieeexplore.ieee.org/document/53070/

14. Sheng Y, Rovnyak SM. Decision Tree-Based Methodology for High Impedance Fault Detection. IEEE Trans Power Deliv [Internet]. 2004 Apr;19(2):533–6. Available from: http://ieeexplore.ieee.org/document/1278405/

15. Vasca F, Iannelli L. Dynamics and Control of Switched Electronic Systems. Springer, editor. 2012.

16. Pola G, Bujorianu ML, Lygeros J, Di Benedetto MD. Stochastic Hybrid Models: An Overview. IFAC Proc Vol [Internet]. 2003 Jun;36(6):45–50. Available from: http://dx.doi.org/10.1016/S1474-6670(17)36405-4

17. Hu J, Lygeros J, Sastry S. Toward Stochastic Hybrid System. Available from: http://sec.eecs.berkeley.edu/papers/99/StoHyb/StoHyb.pdf

18. Lygeros J, Prandini M. Stochastic Hybrid Systems: A Powerful Framework for Complex, Large Scale Applications. Eur J Control [Internet]. 2010 Jan;16(6):583–94. Available from: http://dx.doi.org/10.3166/ejc.16.583-594

19. Iurinic LU, Herrera-Orozco AR, Ferraz RG, Bretas AS. Distribution Systems High-Impedance Fault Location: A Parameter Estimation Approach. IEEE Trans Power Deliv [Internet]. 2016 Aug;31(4):1806–14. Available from: http://ieeexplore.ieee.org/document/7355370/

20. Suteerawatananon S, Chompusri Y, Charbkaew N, Bunyagul T. Design of a Low Cost Microcontroller Based High Impedance Fault Detector. In: 2018 15th International Conference on Electrical Engineering/Electronics, Computer, Telecommunications and Information Technology (ECTI-CON) [Internet]. IEEE; 2018. p. 552–5. Available from: https://ieeexplore.ieee.org/document/8619950/

21. Dash DK, Biswal T, Swain SC. Optimum Relaying Scheme of High Impedance Fault Detection in Micro-Grid. In: 2020 National Conference on Emerging Trends on Sustainable Technology and Engineering Applications (NCETSTEA) [Internet]. IEEE; 2020. p. 1–6. Available from: https://ieeexplore.ieee.org/document/9119919/

22. Nayak PK, Sarwagya K, Biswal T. A novel high impedance fault detection technique in distribution systems with distributed generators. In: 2016 National Power Systems Conference (NPSC) [Internet]. IEEE; 2016. p. 1–6. Available from: http://ieeexplore.ieee.org/document/7858855/

doi: 10.25100/iyc.v26i3.14343

23. Yong H, Minyou C, Jinqian Z. High impedance fault identification method of the distribution network based on discrete wavelet transformation. In: 2011 International Conference on Electrical and Control Engineering [Internet]. IEEE; 2011. p. 2262–5. Available from: http://ieeexplore.ieee.org/document/6057329/

24. Gautam S, Brahma. Detection of High Impedance Fault in Power Distribution Systems Using Mathematical Morphology. IEEE Trans Power Syst [Internet]. 2013 May;28(2):1226–34. Available from: http://ieeexplore.ieee.org/document/6311450/

25. Zamanan N, Sykulski J. The evolution of high impedance fault modeling. In: 2014 16th International Conference on Harmonics and Quality of Power (ICHQP) [Internet]. IEEE; 2014. p. 77–81. Available from: http://ieeexplore.ieee.org/document/6842852/

26. Cui Q, Weng Y. Enhance High Impedance Fault Detection and Location Accuracy via -PMUs. IEEE Trans Smart Grid [Internet]. 2020 Jan;11(1):797–809. Available from: https://ieeexplore.ieee.org/document/8755317/

27. Khoshkhoo H, Sadeghi SHH, Moini R, Talebi HA. An efficient power control scheme for electric arc furnaces using online estimation of flexible cable inductance. Comput Math with Appl [Internet]. 2011 Dec;62(12):4391–401. Available from: http://dx.doi.org/10.1016/j.camwa.2011.10.009

28. Nikolaev AA, Tulupov PG, Savinov DA. Statistical analysis of random fluctuations of currents in the electric arc steel-making furnace for different melting techniques. In: 2017 International Conference on Industrial Engineering, Applications and Manufacturing (ICIEAM) [Internet]. IEEE; 2017. p. 1–7. Available from: http://ieeexplore.ieee.org/document/8076206/

29. Toda M. On the Theory of the Brownian Motion. J Phys Soc Japan [Internet]. 1958 Nov;13(11):1266–80. Available from: https://journals.jps.jp/doi/10.1143/JPSJ.13.1266

30. Iula A, Cerro D, Pappalardo M, Lamberti N. FEA and experimental characterization of langevin transducers with comparable longitudinal and lateral dimensions. In: IEEE Ultrasonics Symposium, 2004 [Internet]. IEEE; 2004. p. 650–3. Available from: http://ieeexplore.ieee.org/document/1417808/

31. Vasicek O. An equilibrium characterization of the term structure. J financ econ [Internet]. 1977 Nov;5(2):177–88. Available from: https://linkinghub.elsevier.com/retrieve/pii/0304405X77900162

32. Bibbona E, Panfilo G, Tavella P. The Ornstein–Uhlenbeck process as a model of a low pass filtered white noise. Metrologia [Internet]. 2008 Dec;45(6):S117–26. Available from: https://iopscience.iop.org/article/10.1088/0026-1394/45/6/S17

33. Svoboda S. The Vasicek Model. In: Interest Rate Modelling [Internet]. London: Palgrave Macmillan UK; 2004. p. 3–17. Available from: http://link.springer.com/10.1057/9781403946027_1

34. Rößler A. Runge–Kutta Methods for the Strong Approximation of Solutions of Stochastic Differential Equations. SIAM J Numer Anal [Internet]. 2010 Jan 1;48(3):922–52. Available from: http://epubs.siam.org/doi/10.1137/09076636X

doi: 10.25100/iyc.v26i3.14343

35. Maximov S, Torres V, Ruiz HF, Guardado JL. Analytical Model for High Impedance Fault Analysis in Transmission Lines. Math Probl Eng [Internet]. 2014;2014:1–10. Available from: http://www.hindawi.com/journals/mpe/2014/837496/

36. Elkalashy NI, Lehtonen M, Darwish HA, Izzularab MA, Taalab AI. Modeling and Experimental Verification of a High Impedance Arcing Fault in MV Networks. In: 2006 IEEE PES Power Systems Conference and Exposition [Internet]. IEEE; 2006. p. 1950–6. Available from: http://ieeexplore.ieee.org/document/4076038/

37. Sedighi AR, Haghifam MR. Simulation of high impedance ground fault In electrical power distribution systems. In: 2010 International Conference on Power System Technology [Internet]. IEEE; 2010. p. 1–7. Available from: http://ieeexplore.ieee.org/document/5666061/

38. Costa FB, Souza BA, Brito NSD, Silva JACB, Santos WC. Real-Time Detection of Transients Induced by High-Impedance Faults Based on the Boundary Wavelet Transform. IEEE Trans Ind Appl [Internet]. 2015 Nov;51(6):5312–23. Available from: http://ieeexplore.ieee.org/document/7110357/

39. Embrechts P, Herzberg AM, Kalbfleisch HK, Traves WN, Robertson Whitla J. An introduction to wavelets with applications to Andrews; plots. J Comput Appl Math [Internet]. 1995 Nov;64(1–2):41–56. Available from: https://linkinghub.elsevier.com/retrieve/pii/0377042795000054

40. Solanki M. Transient protection of transmission line using wavelet transform. In: 7th International Conference on Developments in Power Systems Protection (DPSP 2001) [Internet]. IEE; 2001. p. 299–302. Available from: https://digital-library.theiet.org/content/conferences/10.1049/cp_20010159

doi: 10.25100/iyc.v26i3.14343